Proceedings of the 2016 International Conference on Industrial Engineering and Operations Management
Kuala Lumpur, Malaysia, March 8-10, 2016

Geometric Chip Analysis of Helical End Milling Based on a Variable Flow Stress Machining Theory

Majed Masmali and Philip Mathew
School of Mechanical and Manufacturing Engineering
The University of New South Wales
Sydney, Australia

***Abstract*—This paper will present a developed model to predict cutting forces in flat helical end milling based on a variable flow stress machining theory. A chip geometry model is divided into a number of segments by discretizing the radial depth of cut. The infinitesimal chip geometrical section is considered to be an independent section for analysis. The maximum and minimum chip thicknesses are calculated for each chip segment and the average chip thickness is obtained to compute the cutting results such as forces, etc. The forces are summed for each segment to obtain the total forces acting on the system of the workpiece and the tool. Hence, the chip geometry for each segment is considered to be constant. The variable flow stress machining theory is employed to predict cutting forces in helical end milling process for these segments. Oblique cutting conditions are applied to cater for the chip flow direction due to the helix angle. The cutting forces can be predicted from input data of work material properties, cutter configuration taking into account the cutting conditions. The work material properties are represented by two material constitutive models - the constitutive equation which is modeled by the empirical power law stress-strain relation used by Oxley and his co-workers and a Johnson-Cook constitutive material model. The validation of the proposed model is achieved by correlating the experimental results with the predicted results. The correlation obtained is very encouraging.**

Keywords—chip thickness; helical end milling; Johnson-Cook material model; milling forces; Oxley machining theory

I. INTRODUCTION

Milling is an intermittent material cutting process to remove the material from the workpiece by a single or multi-fluted tool. This machining process in manufacturing is used for creating aerospace structures, moulds and dies as well as thin walled workpieces. In seeking optimisation and efficiency of the milling process there is a need to build a proper model to understand the nature of the milling process. The fundamentals of the milling process are given in references [1-3]. The aspects of this machining application need to be considered when developing a model. The determination of the instantaneous undeformed chip thickness is one of the key issues in the modelling of the milling process to understand the mechanism of material removal. The nature of material removal that occurs when a shaped tool interferes with a layer of material in the workpiece determines the parameters associated with the process. Therefore a proper analysis of chip formation is crucial. It is important to understand how this layer of material is removed in order for modelling approach to be successful. Milling force models can be classified as analytical, artificial Intelligence (AI) based, Finite Element Method (FEM), hybrid, mechanistic and empirical modelling approaches [4-5]. Among these modelling techniques, the analytical modeling approach based on a variable flow stress machining theory will be demonstrated in this paper to predict cutting forces in flat helical end milling process. The description of the Oxley machining theory and its development can be found in references [6-8]. The predictive machining theory is described to consider the variability of the material flow stress with strain, strain-rate and temperature to predict chip geometry, cutting forces etc.

The first attempt to extend Oxley's machining theory towards milling was in 1986 by Young [9-10]. Young's model extended Oxley's machining approach to predict cutting forces in face milling. The varying chip thickness is divided into a series of small radial elements. These chip segments are treated as a constant geometry to be able to demonstrate the variable flow stress machining theory. The comparisons between the results of the proposed model and the measured forces have been found in good agreement with respect to the amplitude and shape of force profiles. The results have found that the force in tangential and radial direction have significant impact with varying range of depth of cut, while the vertical force had not shown any significant effect. Ekanayake and Mathew [11] extended the application of Oxley's machining theory to predict cutting forces in the high speed milling process. The model developed is used to predict forces in high speed milling with two different materials AISI 1045 and AISI 4140. The theoretical model is verified by conducting experimental work. Three types of inserts were used and they are a coated carbide triangular insert with 0.8 mm nose radius, a cermet triangular insert with a chamfered edge and a coated carbide insert with 2 mm nose radius. The output of the model is capable of predicting milling forces. However, this proposed model needs further improvement to predict the forces for different types of materials with different tool configurations. The comparative results showed errors less than 25% for the triangular inserts and with an

error below 50% for 2 mm nose radius insert tool between the predicted and experimental results. The radial and vertical forces can be predicted with less than 60% error.

The application of a variable flow stress machining theory is extended to predict forces in helical end milling by Li *et al.* [12]. In the proposed force model, the helical end mill has been discretised into a number of slices along its axis to cater the helix angle. The force acting on each segment has been summed to compute the total forces acting on the helical end mill cutter. The forces prediction was validated by comparing the simulation results with the experimental values. The material was ASSAB760 plain carbon steel with chemical composition 0.5% Carbon content. The cutter used had four flutes and a 30° helix angle. The maximum percentage error has been found less than 18% for half immersion cases and below 25% in case of full immersion. Masmali and Mathew [13] applied the variable flow stress machining theory to predict milling forces with a non-uniform helix angle tool. The work material properties are represented by two material constitutive models - the material properties for Aluminum developed by Kristyanto which extended Oxley's machining theory to predict forces for Aluminum alloys [14-15] and a Johnson-Cook constitutive material [16] property curve for Al6061 material. The results obtained showed reasonable correlation. However, there is a need to improve the modeling of cutting forces in helical end milling by considering the shape geometry of chip thickness.

It is noted that in the literature there are many ways to define the changing material flow properties in the plastic deformation region. The methodologies have been the use of the MacGregor and Fisher model [17] of velocity modified temperature and the Johnson and Cook model [16] to combine the effects of strain, strain-rate and temperature with a number of parametric variables. The MacGregor and Fisher model combines the effects of temperature and strain-rate into one variable called velocity modified temperature, T_{mod}, and thus one is able to derive material property constants of a material using this variable. The constants which define the equation for flow stress are defined as a function of Tmod. In the Johnson and Cook model, the material properties are derived by using an equation, which has a combined effect from the strain, strain-rate and temperature. Thus one is able to obtain the flow stress of the material for a given strain, strain-rate and temperature. However there is a necessity to derive the constants in the equation for each different material. Therefore it would be advantageous to find out which of the two methods used will be able to predict the forces generated in the end milling process with better accuracy. In this paper a methodology is developed for helical end mills removing the layers of material from a thin-walled section of the workpiece. The main contribution of this paper is to present a different analytical modeling of chip geometry in flat helical end milling process. Second is to compare the results obtained from the two constitutive material models. Experimental work to verify the model is presented as well and the comparison of results given. The conclusion is finally presented. The paper will present some suggestions for future work that is necessary to improve the methodology used.

II. Analytical Modeling of Chip Geometry

As the cutting progresses, the helical cutter is fed into the workpiece to remove away a non-uniform layer of material due to the intermittent process. Based on the direction of the feed motion, the radial cut thickness varies from thick to thin in case of the down milling process or the size of the radial cut thickness starts from zero at the beginning of the interface between the flute and the workpiece to a maximum before disengaging in the case of up milling process. The variation of width of cut thickness is considered in this paper.

A. Theoretical Model

To demonstrate the use of the variable flow stress machining theory to predict the milling forces in helical end milling process, the following assumptions are made. The non-uniform chip thickness geometry is divided into a number of segments based on the radial depth of cut as shown in Fig. 1. The individual chip geometrical section is considered to be an independent element for analysis. The radial depth of cut (r_d) is divided into equal number of segments and Δr_d is the size of discrete width of cut as in (1). The segments are determined arbitrarily by the authors to determine the number for analysis (say 5 segments).

$$\Delta r_d = \frac{r_d}{segments} \tag{1}$$

For the down milling process, as the flute engages to remove the material at maximum thickness at the beginning of the cut and gradually decreases to zero as the flute rotates to cut away a layer of material as shown in Fig. 2. Therefore, the value of the radial depth of cut decreases with respect to each chip segment as shown in (2).

$$r_{d(i)} = \sum_{i=1}^{Nseg} \left(r_{d(i)} - \Delta r_d \right) \tag{2}$$

where N_{seg} is the total number of segments

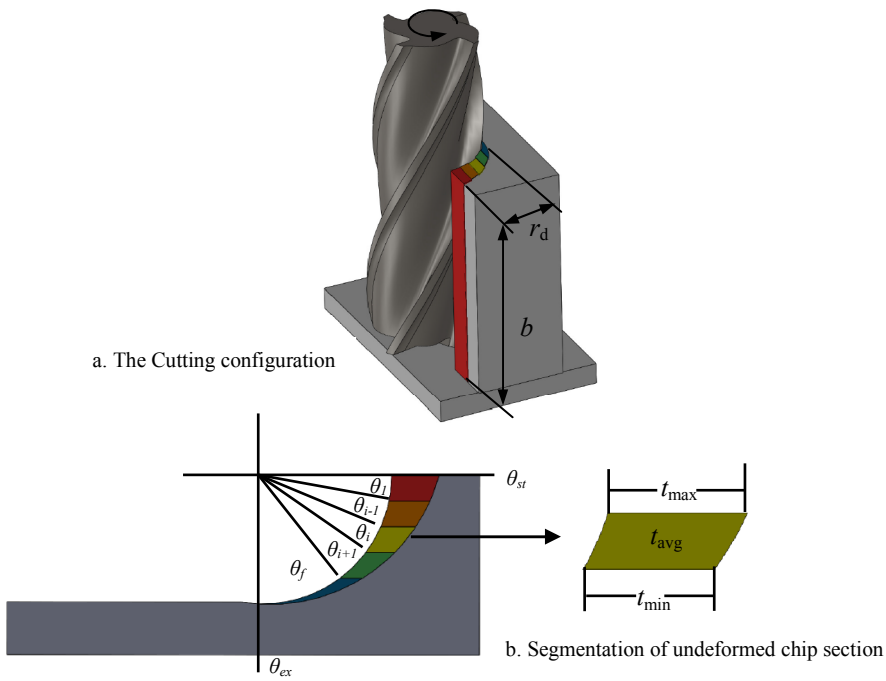

Fig. 1. The proposed model for analysis

Therefore, the maximum chip thickness for each chip segment is computed as in (3) based on the current width of cut (r_d), feed per tooth (f_t) and the cutter diameter (D_C):

$$t_{max(i)} = 2 f_t \sqrt{\frac{r_{d_{(i)}}}{D_C}\left(1 - \frac{r_{d_{(i)}}}{D_C}\right)} \tag{3}$$

While, the minimum chip thickness for each chip element can be obtained based on the width of cut and subtracting the discretized size of the width of cut from the original width of cut as given in (4).

$$t_{min(i)} = 2 f_t \sqrt{\left(\frac{r_{d_{(i)}} - \Delta r_d}{D_C}\right)\left(1 - \frac{r_{d_{(i)}} - \Delta r_d}{D_C}\right)} \tag{4}$$

The immersion angle for each chip segment can be computed as follows. While the start angle θ_{st} depends on the radial depth of cut (r_d) and the tool radius (R_C) and is obtained as in (5).

$$\theta_{st(i)} = 180 - \cos^{-1}\left(\frac{R_C - r_{d_{(i)}}}{R_C}\right) \tag{5}$$

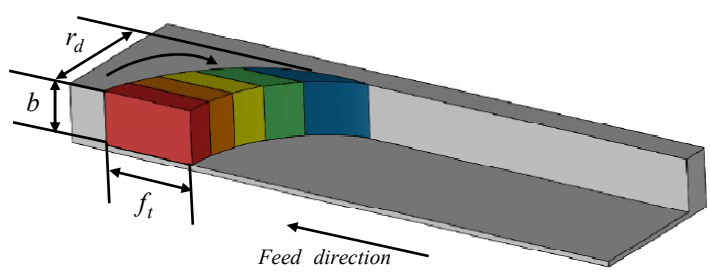

Fig. 2. Geometry of the down milling process

The exit angle $\theta_{ex(i)}$ for each segment can be computed as in (6) with all other terms defined before.

$$\theta_{ex(i)} = 180 - cos^{-1}\left(\frac{R_C - (r_{d_{(i)}} - \Delta r_d)}{R_C}\right) \tag{6}$$

In case of up milling process, the radial cut thickness increases from zero at the beginning of the interface between the cutter and workpiece to a maximum when flute disengagement occurs as shown in Fig. 3. Therefore, the value of the width of cut increases incrementally based on the size of the width cut segment as in (7).

$$r_{d(i)} = \sum_{i=1}^{Nseg}(i \times \Delta r_d) \tag{7}$$

The minimum chip thickness for the first segment is zero. For each subsequent chip segment the minimum chip thickness is the maximum of the previous segment ($i - 1$). Based on this increment the various chip thicknesses of each segment can be calculated. $t_{min(i)}$ as given by (8).

$$t_{min(i)} = 2f_t\sqrt{\left(\frac{r_{d_{(i)}} - \Delta r_d}{D_C}\right)\left(1 - \frac{r_{d_{(i)}} - \Delta r_d}{D_C}\right)} \tag{8}$$

While, the maximum chip thickness for each infinitesimal chip element is given based on the width of size as in (9).

$$t_{max(i)} = 2f_t\sqrt{\frac{r_{d_{(i)}}}{D_C}\left(1 - \frac{r_{d_{(i)}}}{D_C}\right)} \tag{9}$$

The start angle, $\theta_{st(i)}$ in case of up milling mode is zero at the beginning of the tooth engagement when considering the first segment. Subsequent segments have a start angle given by (10).

$$\theta_{st(i)} = cos^{-1}\left(\frac{R_C - (r_{d_{(i)}} - \Delta r_d)}{R_C}\right) \tag{10}$$

While, the exit angle, $\theta_{ex(i)}$ for each segment can be computed as in (11).

$$\theta_{ex(i)} = cos^{-1}\left(\frac{R_C - r_{d_{(i)}}}{R_C}\right) \tag{11}$$

Once the maximum and minimum chip thicknesses are identified for each chip element, this leads to the average chip thickness which is computed as shown in (12).

$$t_{avg} = \frac{t_{max} + t_{min}}{2} \tag{12}$$

The value of t_{avg} is used in the Oxley Machining Theory to calculate the predicted values of forces and t_{avg} is defined as t_1 (uncut chip thickness) in this model. Once the constant geometry for each chip segment is obtained it allows the use of the variable flow stress machining theory to determine the forces, etc. by analysing the chip formation process.

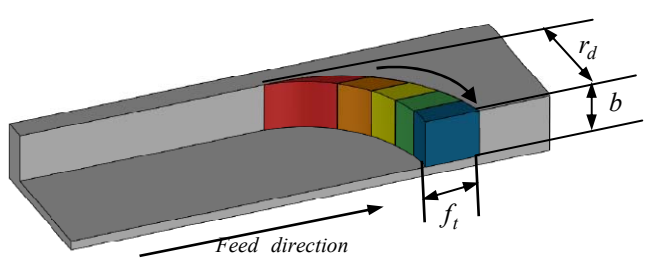

Fig. 3. Geometry of the up milling process

B. Orthogonal Cutting Condition

The orthogonal machining condition is applied to each chip segment to calculate the cutting force (F_C) and thrust force (F_T). The inclination angle in case of two dimensional orthogonal cutting is zero [6-8]. The orthogonal chip formation model is shown in Fig. 4. In order to determine the shear angle (ϕ), it is important that the resultant force generated at the shear plane is equal to the resultant force generated at the tool-chip interface and the temperature determination at the different zones must converge during this computational process. For temperature calculations, the shear zone temperature factor and tool-chip interface temperature factor are set to be 0.7 for 0.2%C plain carbon steel [6].

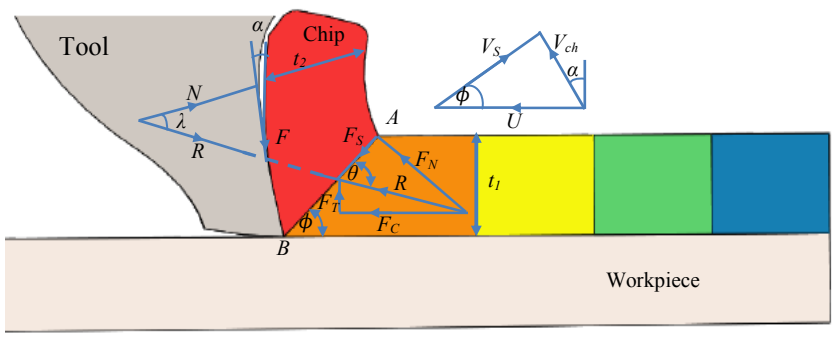

Fig. 4. Orthogonal chip formation model

For steady state machining the average shear stress at tool chip interface must be equal to the average shear flow stress at tool-chip interface ($\tau_{int} = k_{chip}$) for a given value of shear angle, ϕ [6] for equilibrium of resultant forces from the shear plane and tool/chip interface. Once the equilibrium is achieved then the cutting forces can be evaluated. A numerical iterative method is employed for this purpose. The calculation of the values for both the AB plane and tool-chip interface are carried out. Once, the shear angle is determined, the chip thickness (t_2) and the various force components for the two dimensional flow can be obtained for each chip segment as expressed in (13–20).

$$t_2 = \frac{t_1 \cos(\phi - \alpha)}{\sin(\phi)} \tag{13}$$

$$R = \frac{k_{AB}\, t_1 w}{\sin(\phi)\cos(\theta)} \tag{14}$$

$$F_C = R\cos(\lambda - \alpha) \tag{15}$$

$$F_T = R\sin(\lambda - \alpha) \tag{16}$$

$$F = R\sin\lambda \tag{17}$$

$$N = R\cos\lambda \tag{18}$$

$$V_{ch} = \frac{\sin(\phi)}{\cos(\phi - \alpha)} \tag{19}$$

$$V_s = \frac{U\cos(\alpha)}{\cos(\phi - \alpha)} \tag{20}$$

where t_2, R, N, λ, α, V_{ch}, V_s, F_N, F_S and k_{AB} are the chip thickness, the resultant force, normal force at the tool/chip interface, the friction angle, the rake angle, chip velocity, the shear velocity on plane AB, normal force to AB, shear force on AB and shear flow stress on AB respectively. From the results of orthogonal cutting condition, it is now possible to determine the three dimensional forces acting on the chip segment by extending the analysis to the oblique machining condition.

C. Oblique Cutting Condition

The helical cutting edge of the cutter is not orthogonal to the cutting velocity direction and it corresponds to the inclination cutting edge angle in the oblique cutting process [18-22]. Therefore, the three dimensional cutting process is applied to predict the third cutting force component [23-24]. In addition, oblique cutting conditions are employed to cater for the chip flow direction due to the effect of the helix angle.

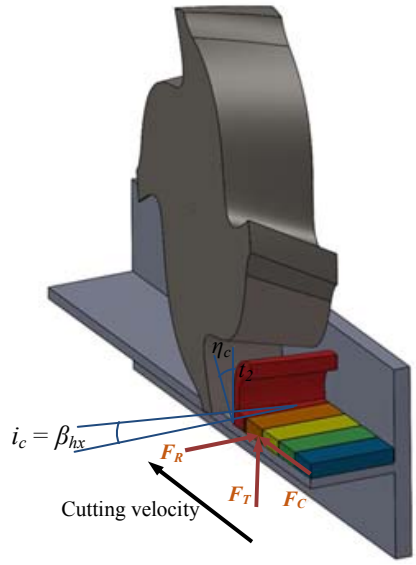

Fig. 5. Oblique chip formation model

To further simplify the model, the assumption that the chip segment does not change widthwise is made. Therefore, the chip flow angle is considered to be equal to the angle of obliquity as in (21) according to Stabler's chip flow law [25].

$$\eta_c = i_c \tag{21}$$

The third force component as shown in (22) represents the radial force acting in Fig. 5.

$$F_R = \frac{Fc\left(\sin i_c - \cos i_c \sin\alpha \tan\eta_c\right) - F_T\left(\cos\alpha \tan\eta_c\right)}{\sin i_c \sin\alpha \tan\eta_c + \cos i_c} \tag{22}$$

Based on the above assumption, the inclination angle (i_c) is assumed to equivalent to the helix angle (β_{hx}) and chip flow angle (η_c). Therefore, (22) for the radial force component can be rewritten as in (23).

$$F_R = \frac{Fc\left(\sin\beta_{hx} - \cos\beta_{hx}\sin\alpha\tan\beta_{hx}\right) - F_T\left(\cos\alpha\tan\beta_{hx}\right)}{\sin\beta_{hx}\sin\alpha\tan\beta_{hx} + \cos\beta_{hx}} \tag{23}$$

D. Force Predictions

Equation (24) expresses the angular position and the symbols (*i, j, k, l*) are representing the rotational increment index (*i*), the index of the flute (*j*), the discrete axial depth of cut index (*k*) and the chip segment index (*l*) respectively, as shown in Fig. 6.

$$\theta_{ijkl} = \left(\Delta\theta\right)\cdot i - \left(\frac{2\pi}{N_f}\right)\cdot j - \left(\frac{\Delta b}{R_C}\tan\beta_{hx}\right)\cdot k \tag{24}$$

where $\Delta\theta$ is the angular increment, Δb is the discrete axial depth of cut as outlined in[2-3] and N_f is the number of helical flutes. The differential milling forces are subjected to the cutter flute numbers, the axial segment numbers, the chip segment numbers and helical cutter rotation angle as given in (25 - 27).

$$\Delta F_{x(i,j,k,l)} = \Delta F_C \cos\theta_{ijkl} + \Delta F_T \sin\theta_{ijkl} \tag{25}$$

$$\Delta F_{y(i,j,k,l)} = -\Delta F_C \sin\theta_{ijkl} + \Delta F_T \cos\theta_{ijkl} \tag{26}$$

$$\Delta F_{z(i,j,k,l)} = -\Delta F_{R_{ijkl}} \tag{27}$$

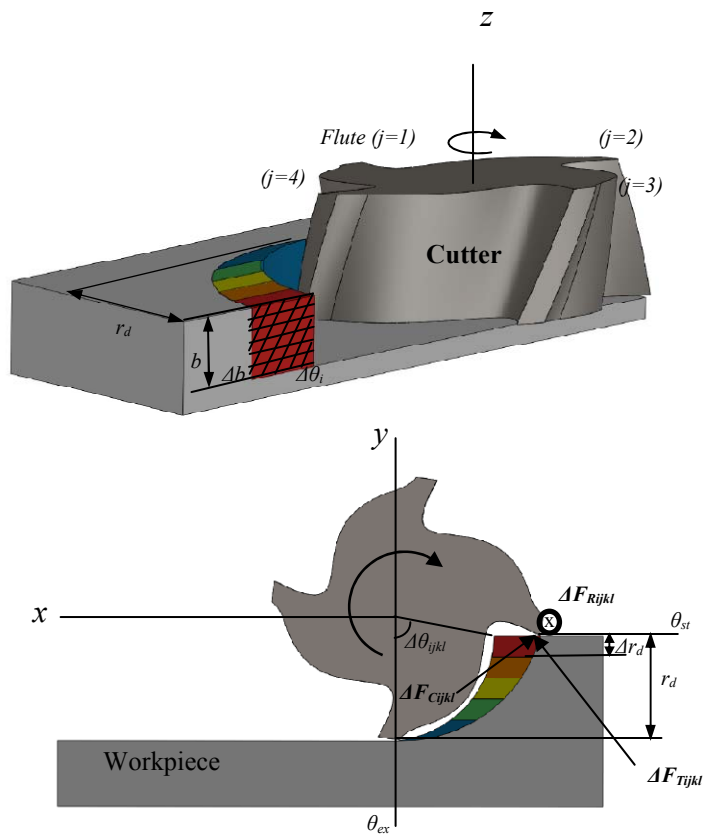

Fig. 6. Differential milling forces applied on an helical end mill

Finally, the total cutting forces in X, Y and Z directions at a given rotational position can be computed as in (28-30).

$$F_X = \sum_{i=1}^{i}\sum_{j=1}^{j}\sum_{k=1}^{k}\sum_{l=1}^{l} \Delta F_{x(i,j,k,l)} \tag{28}$$

$$F_Y = \sum_{i=1}^{i}\sum_{j=1}^{j}\sum_{k=1}^{k}\sum_{l=1}^{l} \Delta F_{y(i,j,k,l)} \tag{29}$$

$$F_Z = \sum_{i=1}^{i}\sum_{j=1}^{j}\sum_{k=1}^{k}\sum_{l=1}^{l} \Delta F_{z(i,j,k,l)} \tag{30}$$

III. Work Material

The chemical composition for 0.2% C plain carbon steel is given in Table I.

TABLE I. Chemical Composition of AISI 1020[26]

Element	***Carbon***	***Silicon***	***Sulfur***	***Manganese***	***Aluminum***
Content	0.20%	0.15%	0.015%	0.72%	0.015%

The thermo physical properties for work material are the density, specific heat and thermal conductivity. The thermal properties of 0.2% C plain carbon steel are listed in Table II where *T* is the temperature of the material when it is worked on by the process.

TABLE II. THERMO-PHYSICAL PROPERTIES OF 0.2% PLAIN CARBON STEEL [26]

Specific Heat (J/(kg K))	S = 420 + 0.504T
Thermal Conductivity (W/m K)	K = 54.17 + 0.0298T
Density (kg / m^3)	7862
Melting Temperature (°C)	1460

IV. CONSTITUTIVE EQUATIONS

To describe the material behaviour during machining, the two constitutive equations are addressed to represent the plastic deformation occurring at high strain, strain rate and temperature. These two constitutive equations are the constitutive equation which is modeled by the empirical power law stress-strain relation used by Oxley and co-workers [6], and a Johnson-Cook constitutive material model [16].

A. Empirical Power Law Stress Strain Curve

The power law stress-strain relation is used in the Oxley model to represent the changing flow stress conditions and is expressed as in (31).

$$\sigma = \sigma_1 \varepsilon^n \tag{31}$$

where σ is the flow stress for a given value of strain ε and σ_1 and n are material constants for a given temperature and strain-rate. These values change with different temperatures and strain-rates. The MacGregor and Fisher model combines the effects of temperature and strain-rate into one variable called velocity modified temperature, T_{mod}, and thus one is able to derive material property constants of a material using this variable [17]. The constants, σ_1 and n in (31) which define the equation for flow stress are defined as a function of T_{mod} as given in (32).

$$T_{mod} = T\left(1 - \upsilon \log \frac{\dot{\varepsilon}}{\dot{\varepsilon}_o}\right) \tag{32}$$

where T is the temperature, $\dot{\varepsilon}$ is the direct strain-rate, and υ are $\dot{\varepsilon}_o$ constants assumed to be 0.09 and 1s^{-1} respectively.

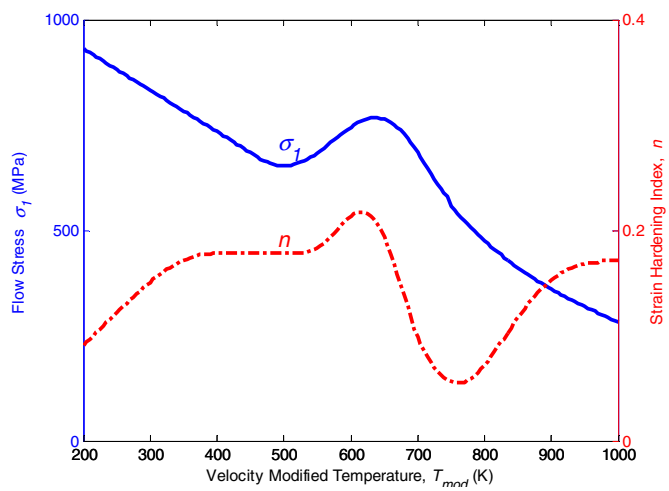

Fig. 7. Variation of flow stress and strain hardening index with velocity modified temperature

Fig. 7 presents the shape of the σ_1 and n curves for 0.2% plain carbon steel. It can be seen that the flow stress σ_1 decreases with increasing the temperature. It can be also noticed that the strain hardening index n remains constant over the T_{mod} range between 400 °K and 550 °K.

B. Johnson-Cook Constitutive Model

The Johnson-Cook constitutive material model in which the constants are available for most commonly machined materials is adopted in this research to represent the material flow stress under different cutting conditions. Adibi-Sedeh et al. [27], and Lalwani et al. [28] extended Oxley's machining theory with Johnson-Cook material model. The constitutive equation for a material can be expressed as an equation relating flow stress with temperature, strain and strain rate [16]. The general structure of Johnson-Cook material model is given by (33).

$$\sigma = \left(A + B\varepsilon^n\right)\left(1 + Cln\frac{\dot{\varepsilon}}{\dot{\varepsilon}_o}\right)\left(1 - \left(\frac{T - T_w}{T_m - T_w}\right)^m\right) \tag{33}$$

where, *A, B, n, C* and m are the five parameters of the Johnson-Cook constitutive equation where *A* is the quasi-static yield strength, *B* the coefficient of strain hardening, *n* the exponent of strain hardening, *C* the coefficient of strain rate sensitivity, *m* the coefficient of temperature sensitivity. *T* is the instantaneous temperature of the material, Tm is the melting temperature of the material, T_w is the initial work temperature, ε is the strain, $\dot{\varepsilon}$ is the strain rate and $\dot{\varepsilon}_o$ is reference strain rate. The parameters for Johnson-Cook material model of 0.2%C plain carbon steel are listed in Tables III.

TABLE III. JOHNSON AND COOK PARAMETERS OF 0.2%C PLAIN CARBON STEEL [16]

Parameters	A	B	C	m	n
Value	350 (MPa)	275 (MPa)	0.022	1.00	0.36

Due to the similarity of chemical compositions and the percentage of carbon in the compositions of AISI 1006 and AISI 1020, the Johnson-Cook parameters for AISI 1006 are used to represent the flow stress of AISI 1020 in this study. However, the Johnson-Cook parameters for AISI 1006 did not allow convergence for the machining solution for the cutting conditions used in this study. A further modification to Johnson-Cook parameters is employed in this study. The exponent of strain hardening parameter is modified from 0.36 to 0.116 based on the strain hardening index results from Oxley material model for the same material. This value of *n* is used for Johnson-Cook strain hardening index while other parameters are assumed to be constant. The use of n = 0.116 allowed solutions to be obtained for the cutting conditions used here. It should be noted that strain hardening index in (31) and Johnson-Cook strain hardening index are different.

V. EXPERIMENTAL WORK

To verify the numerical model, the experimental work is performed on a Deckel Maho 5-axis CNC machining centre using the experimental setup as shown in Fig. 8. The signals were acquired simultaneously and their sampling rate was set as 8,000 Hz. The cutting force signals in x (Fx), y (Fy) and z (Fz) directions were measured by a three component Kistler dynamometer type 9257B, which was connected to a multi-channel charge Kistler amplifier type 5070 and the output signal was acquired by a DynoWare DAQ system type 5697. The cutting conditions are listed in Table IV. The cutting conditions were selected to determine the effect of cutting forces on thin wall deflections and as such the speeds, feeds and depths of cut selected showed the change in forces for the changing cutting parameters. The experiments were carried out on a thin wall, which is 60 mm long and the results of the experimental work are taken at a random sample of three revolutions. The results were consistent along the full test.

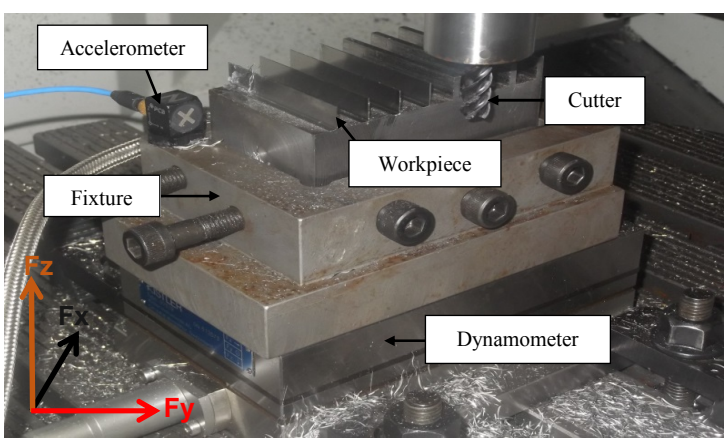

Fig. 8. Experimental set-up

The experiments were carried out using solid carbide end mills. The milling cutter used with 10 mm in diameter, four fluted with a 50° helix angle and 0° rake angle.

TABLE IV. CUTTING CONDITIONS

Cutting speed (m/min)	50	70	90	110
Feed rate (mm/tooth)	0.04	0.06	0.08	0.10
Axial depth of cut (mm)	10	15	20	
Radial depth of cut (mm)	0.5			

The size of the workpiece is 100 x 60 x 60 mm^3. The workpiece is designed to have eight ribs (thin-walls) with the gap between the ribs being 10.1 mm for the tool path as the diameter of the cutter is 10 mm. The thickness of each rib is 3 mm. The height of the wall is 20 mm, 15 mm and 10 mm according to the axial depth of cut to be used for milling.

VI. RESULTS AND DISCUSSION

The comparison between the experimental and predicted milling force waveforms along the feed (Fx), normal to feed (Fy) and axial (Fz) directions over three cutter revolutions are presented in Figs. 9 and 10. It can be seen that there are peak values which corresponds to the flutes engaging with work material. The forces increase fairly quickly for Fx, but gradually for Fy when the tool engages with the workpiece. Then, the peak force decreases until the flute disengages from the workpiece. Fz has a higher variability which could be due to the vibrations that occur during the milling process.

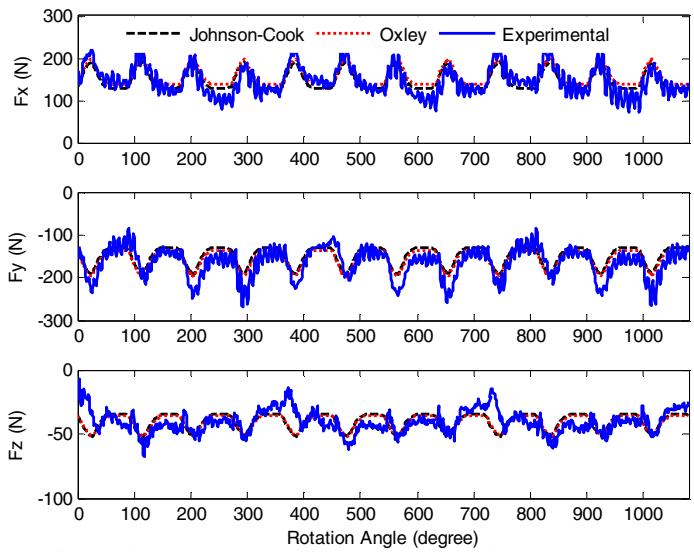

Fig. 9. Predicted and measured down milling forces with angular tool rotation (in three revolutions)
(Cutting Conditions; speed: 50m/min, feed: 0.04mm/tooth, width: 0.50mm, depth: 15mm)

Fig. 9 presents the measured and predicted cutting force waveforms for down milling with respect to following cutting conditions- cutting speed 50 m/min, the axial depth of cut 15mm, the radial depth of cut 0.5 mm and the feed 0.04 mm/tooth. It can be seen that the predicted values for both the flow stress material models show good agreement with respect to the milling forces pattern and the peak to peak amplitude values.

It is observed that there is a slight difference between these two constitutive material models however it is not worth worrying about for the results seen here. However, there are clear differences between the values of measured forces and the model results. The measured force distributions fluctuate for a tooth pass and it is repeated for each cutter rotation angle. The explanation of the non-uniform distribution with the peak values of the milling forces are probably due to the tool runout. The current model does not take into account the phenomena of cutter runout.

Fig. 10 presents the measured and predicted cutting force waveforms along the feed (Fx), normal to feed (Fy) and axial (Fz) directions over three cutter revolutions for up milling using the following cutting conditions - cutting speed 50 m/min, the axial depth of cut 10 mm, the radial depth of cut 0.5 mm and the feed 0.08 mm/tooth. It can be seen that the experimental and predicted values follow similar cutting force profiles and the differences between the forces that are predicted using Johnson-Cook constitutive model and Oxley flow stress properties are considerably small. Overall, the proposed model shows good results when compared to the simulated values.

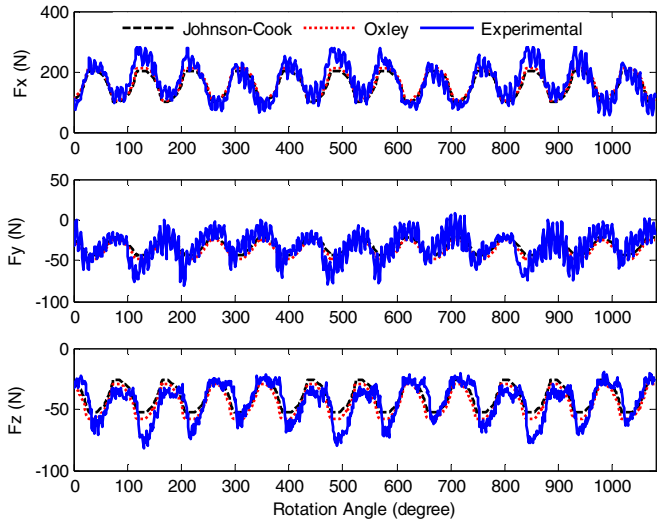

Fig. 10. Predicted and measured up milling forces with angular tool rotation (in three revolutions)
(Cutting Conditions; speed: 50m/min, feed: 0.08mm/tooth, width: 0.50mm, depth: 10mm)

Furthermore, the assumptions made for the flow stress parameters in the Johnson-Cook constitutive model using modification to exponent of strain hardening parameter from 0.36 to 0.116 based on the strain hardening index results from Oxley material model for the same material as outlined in Section IV has enabled predictions for Johnson-Cook material model. This modification to Johnson-Cook constitutive model show reasonable results with the milling test values. Also, it indicates good correlation with the numerical model based on the empirical power stress-strain relation based on the velocity modified temperature concept of MacGregor and Fisher [17] which is modeled by the Oxley and his co-workers [6]. However, any minor differences can be attributed to the dynamic characteristics of the machining process, which results from tool-workpiece interaction. In addition, the change in the signal characteristics of the experimental data may be caused by tool runout as indicated by repeated flute pattern observed in the experimental results. Further, the contact length of tool with workpiece may contribute to the variation of the measured force signals. The comparison between the two flow stress models used show good agreement except in the normal force where there is a slight difference. This may due to the assumption of the flow stress parameters used for the two constitutive models. Overall, the differences seen between the two predicted curves are small and thus it is possible to use either of the material property curves for this 0.2%C plain carbon steel. These results are encouraging for future research into the behaviour of materials under thin walled machining conditions.

VII. Conclusion

The analysis takes into account the variation in uncut chip thickness and the use of two different flow stress property curves. The predicted values gives the deterministic variation of the cutting forces during the milling process and the results follow the trend observed experimentally. These results are encouraging in taking this research further to obtain the dynamic characteristics of vibration and wall deflections. This work is the next stage of the research currently being carried out.

It is important to point out that there are the limitations to this study. The cutting condition used in this research is limited in terms of the radial depth of cut. It is set at 5% low radial immersion indicating a low radial depth of cut for material removal. The full immersion and half immersion cuts were not considered in the present research. Furthermore, tool run-out is not addressed in this research as well as tool wear. However in this work the cutting times involved were very short and thus the effect of tool wear is insignificant. This area of work needs some investigation. The work here only considered flat end milling operation with low radial immersion. There are many types of end milling cutters with different cutting shapes. It is recommended that work to be considered for these different types of end mills. In addition with advent of miniaturisation it is expected more micro-milling operations will be carried out and it is recommended to investigate the micro-milling operation using the variable flow stress machining theory. Cutter run-out is not considered in this research and it may be necessary to consider cutter runout to improve the results obtained especially in the case of wall deflections.

Further suggestion for the future work is the possibility of applying stochastic modelling approach to predict milling forces based on the variable flow stress machining theory. The advantage of the stochastic modelling is that it takes the dynamic nature of the milling process into account as the cutting progresses and therefore may achieve better results. The Johnson-Cook material model in this work had the strain hardening index, *n* assumed as 0.116 for determining the flow stress property to

predict the cutting forces for 0.2% carbon steel. Therefore further work is needed to provide accurate coefficients that are able to predict forces for different cutting conditions for the Johnson-Cook material model.

REFERENCES

[1] E. J. A. Armarego and R. H., Brown, "The Machining of Metals," Prentice Hall, Englewood Cliffs, New Jersey, 1969.

[2] G. Tlusty, " Manufacturing Process and Equipment," Prentice Hall, Upper Saddle River, New Jersey, 2000.

[3] Y. Altintas, "Manufacturing Automation: Metal Cutting Mechanics, Machine Tool Vibrations and CNC Design," Cambridge: Cambridge University Press, 2000.

[4] W. Grzesik, "Advanced Machining Processes of Metallic Materials," Elsevier, Oxford, UK, 2008.

[5] P. J. Arrazola, T. Özel, D. Umbrello, M. Davies, and I. S. Jawahir, "Recent advances in modelling of metal machining processes," CIRP Annals - Manufacturing Technology, vol. 62, no. 2, pp. 695–718, Jan. 2013.

[6] P. L. B. Oxley, "Mechanics of machining: An analytical approach to assessing machinability," Ellis Horwood Ltd, Chichester, UK, 1989.

[7] P. L. B. Oxley, "Development and application of a predictive machining theory," *Machining Science and Technology*, vol. 2, no. 2, pp. 165–189, Dec. 1998.

[8] J. A. Arsecularatne and P. Mathew, "The Oxley modeling approach, its applications and future directions," *Machining Science and Technology*, vol. 4, no. 3, pp. 363–397, Nov. 2000.

[9] H. T. Young, "Application of predictive machining theory to more complicated processes including single-point oblique cutting tools with other than single straight cutting edges and milling, and experimental verification," Ph.D. dissertation, The University of New South Wales, Sydney, Australia, 1986.

[10] H. T. Young, P. Mathew, and P. L. B. Oxley, "Predicting cutting forces in face milling," *International Journal of Machine Tools and Manufacture*, vol. 34, no. 6, pp. 771–783, Aug. 1994.

[11] R. A. Ekanayake, P. Mathew, "Force predictions for tooling speed limits in end milling using a variable flow stress machining theory," *Proceedings of the 36th North American Manufacturing Research Conference,* Monterrey, Mexico, pp. 429–436, May 20-23, 2008.

[12] H. Z. Li, W. B. Zhang, and X. P. Li, "Modelling of cutting forces in helical end milling using a predictive machining theory," *International Journal of Mechanical Sciences*, vol. 43, no. 8, pp. 1711–1730, Aug. 2001.

[13] M. Masmali, P. Mathew, "Variable flow stress machining theory applied to predict cutting forces in end milling with a variable helix angle end mills," *Proceedings of the 1st International Conference on Industrial, Systems and Manufacturing Engineering*, Amman, Jordan, November 11-12, 2014, ISBN 978-9957-469-03-0

[14] B. Kristyanto, "Development of a predictive theory of machining for Aluminium alloys using material's variable flow stress properties," Ph.D. dissertation, The University of New South Wales, Sydney, Australia, 2003.

[15] B. Kristyanto, P. Mathew, and J. A. Arsecularatne, "Development of a variable flow stress machining theory for Aluminium alloys," *Machining Science and Technology*, vol. 6, no. 3, pp. 365–378, Dec. 2002.

[16] G. R. Johnson, W. H. Cook, "A constitutive model and data for metals subjected to large strains, high strain rates and high temperatures, " *Proceedings of the 7th International Symposium on Ballistics*, Hague, Netherlands, pp. 541–547, April 19-21, 1983.

[17] C. W. MacGregor and J. A. Fisher, "A velocity-modified temperature for the plastic flow of metals," *Journal of Applied Mechanics*, vol. 13, pp. 11–16, 1946.

[18] E. J. A. Armarego and R. C. Whitfield, "Computer based modelling of popular machining operations for force and power prediction," *CIRP Annals - Manufacturing Technology*, vol. 34, no. 1, pp. 65–69, Jan. 1985.

[19] E. Budak, "Analytical models for high performance milling. Part I: Cutting forces, structural deformations and tolerance integrity," *International Journal of Machine Tools and Manufacture*, vol. 46, no. 12–13, pp. 1478–1488, Oct. 2006.

[20] B. Li, Y. Hu, X. Wang, C. Li, and X. Li, "An analytical model of oblique cutting with application to end milling," *Machining Science and Technology*, vol. 15, no. 4, pp. 453–484, Oct. 2011.

[21] A. Moufki, D. Dudzinski, and G. Le Coz, "Prediction of cutting forces from an analytical model of oblique cutting, application to peripheral milling of Ti-6Al-4V alloy," *The International Journal of Advanced Manufacturing Technology*, vol. 81, no. 1–4, pp. 615–626, May 2015.

[22] B. Lin, L. Wang, Y. Guo, and J. Yao, "Modeling of cutting forces in end milling based on oblique cutting analysis," *The International Journal of Advanced Manufacturing Technology*, Sep. 2015.

[23] G. C. I. Lin, "Prediction of cutting forces and chip geometry in oblique machining from flow stress properties and cutting conditions," *International Journal of Machine Tool Design and Research*, vol. 18, no. 3, pp. 117–130, Jan. 1978.

[24] E. Usui and M. Masuko, "Analytical prediction of three dimensional cutting process Part 1: Basic cutting model and energy," *Journal of Engineering for Industry*, vol. 100, no. 77, pp. 222–228, 1978.

[25] G. V. Stabler, "The fundamental geomerty of cutting tool," *Proceedings Journal of the Institution of Mechanical Engineers*, vol. 116, pp. 14–26, 1951.

[26] P. Mathew and P. L. B. Oxley , "Predicting the cutting conditions at which built-up edge disappears when machining plain carbon steels,", *Annals of the CIRP,* vol. 29, pp. 11–14, 1980.

[27] A. H. Adibi-Sedeh, V. Madhavan, and B. Bahr, "Extension of Oxley's analysis of machining to use different material models," *Journal of Manufacturing Science and Engineering*, vol. 125, no. 4, pp. 656–666, 2003.

[28] D. I. Lalwani, N. K. Mehta, and P. K. Jain, "Extension of Oxley's predictive machining theory for Johnson and Cook flow stress model," *Journal of Materials Processing Technology*, vol. 209, no. 12–13, pp. 5305–5312, Jul. 2009.